Proceedings of The Magnetized Plasma in Galaxy Evolution
Sep. 27th – Oct. 1st 2004, Jagiellonian University, Kraków, Poland
Eds. K.T. Chyży, K. Otmianowska-Mazur, M. Soida and R.-J. Dettmar

Magnetic Fields and Star Formation

Richard M. Crutcher

University of Illinois, 1002 W. Green St., Urbana, IL 61801 USA

Abstract

Observations of magnetic fields in molecular clouds are essential for understanding their role in the evolution of dense clouds and in the star formation process. I first briefly describe the observational techniques available for such observations – the Zeeman effect, mapping of polarized dust emission, and mapping of linearly polarized line emission. I then describe an exemplar result, for the high-mass star formation region DR21OH. The data are then used to carry out tests of the two extreme paradigms for what drives star formation – magnetic and thermal support with ambipolar diffusion, and compressible turbulence with negligible magnetic fields. The conclusion is that the magnetic support model is consistent with the data, but *both* turbulence and strong magnetic fields are important in the physics of molecular clouds and in the star formation process.

1 Introduction

Observations of magnetic fields in diffuse H I and dense molecular clouds have now become a fairly routine procedure, and many new observational results have been obtained in the last few years. Most progress has been made in mapping polarized emission from dust, but many new Zeeman observations have also been made, together with the first detections of linearly polarized spectral lines. In this article I will review the observational data and focus on one of the main reasons for observing magnetic fields in molecular clouds – to try to understand their role in the formation and evolution of dense clouds and in the star formation process. Understanding star formation is one of the outstanding challenges of modern astrophysics. However, in spite of significant progress in recent years, there remain unanswered fundamental questions about the basic physics of star formation. In particular, what drives the star formation process? The prevailing view has been that self-gravitating clouds are supported against collapse by magnetic fields, with ambipolar diffusion reducing support in cores and hence driving star formation (e.g., Mouschovias & Ciolek 1999, and references therein). The other extreme is that molecular clouds are intermittent phenomena in an interstellar medium dominated by turbulence, and the problem of cloud support for long time periods is irrelevant (e.g., Elmegreen 2000; MacLow & Klessen 2004, and references therein). In this paradigm, clouds form and disperse by the operation of compressible turbulence, with clumps sometimes becoming gravitationally bound. Even if turbulence originally provides support, it dissipates rapidly and the cores collapse to form stars. In this contribution I focus on discussing how observations of magnetic fields can distinguish between and test these models.

2 Observational Techniques

2.1 Zeeman splitting

The Zeeman effect is the only available technique for measuring directly magnetic field strengths in interstellar clouds (e.g., Crutcher et al. 1993). A Stokes V spectrum reveals the sign (i.e., direction) and magnitude of the line-of-sight component B_{los}. By fitting the frequency derivative of the Stokes parameter I spectrum $\mathrm{dI}/\mathrm{d}\nu$ to the observed V spectrum, B_{los} may be inferred. It is possible to correct statistically for the fact that only one component of $\mathbf{B}$ is measured, i.e., $B_{los} = |\mathbf{B}|\cos\theta$. For a large number of clouds whose magnetic fields are randomly oriented with respect to the observed line of sight,

$$\overline{B}_{los} = \int_0^{\pi/2} |\mathbf{B}|\cos\theta\sin\theta d\theta = \frac{1}{2}|\mathbf{B}|. \tag{1}$$

2.2 Polarization of dust emission

Linear polarization of thermal emission from dust grains arises from elongated grains with their short axes aligned, generally with $\mathbf{B}$ (Lazarian 2003). The position angle of maximum emission will be perpendicular to B_{pos}, so maps of polarized dust emission give the morphology of the field on the plane of the sky. Chandrasekhar and Fermi (1953) suggested that analysis of the small-scale randomness of magnetic field lines could yield estimates of the field strengths. Turbulent or MHD-wave motions will lead to irregular magnetic fields, and the stronger the regular field, the more it resists being irregularized by turbulence. They showed that the magnitude of the irregularity of field lines could yield the regular field strength in the plane of the sky:

$$B_{pos} = Q\sqrt{4\pi\rho}\,\frac{\delta V}{\delta\phi} \approx 9.3\sqrt{n(H_2)}\,\frac{\Delta V}{\delta\phi}\ \mu G, \tag{2}$$

where ρ is the gas density, δV is the velocity dispersion, $\delta\phi$ is the dispersion in polarization position angles in degrees, Q is a factor of order unity, $n(H_2)$ is the molecular hydrogen density in molecules cm^{-3}, and $\Delta V = \sqrt{8ln2}\,\delta V$ is the FWHM line width in km s^{-1}. Here we have used $Q = 0.5$, a calibration based on study of simulations of interstellar clouds by Ostriker, Stone, & Gammie (2001), who found that this method could yield reliable results in molecular clouds.

2.3 Spectral-line linear polarization

Linear polarization may also arise in radio-frequency spectral lines formed in the interstellar medium, even when Zeeman splitting is negligible. This Goldreich-Kylafis effect (Goldreich and Kylafis 1981; Kylafis 1983) may be used to probe magnetic field morphologies in molecular clouds. The direction of the polarization can be either parallel or perpendicular to the magnetic field, depending on the relationship between the line of sight, the direction of the magnetic field, and the direction of a velocity gradient that produces the anisotropic line optical depth that is required to produce linear polarization. As is the case for linearly polarized dust emission, the Chandrasekhar-Fermi method may be applied to maps of spectral-line linear polarization to estimate field strengths.

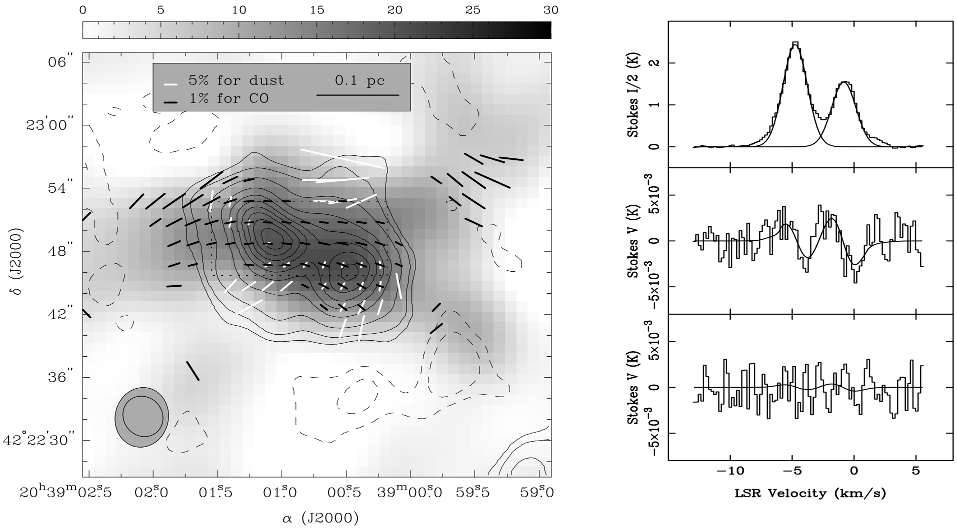

Figure 1: Left: BIMA map of DR21OH (Lai et al. 2003). Contours show the 1.3-mm dust emission, grey scale shows the CO 2-1 line emission integrated over velocity, white line segments show the dust polarization, and black line segments show the CO linear polarization. Right: IRAM 30-m CN 1-0 line profiles toward DR21OH (Crutcher et al. 1999). Observed data are histogram plots, fits are lines. Top panel shows the Stokes I spectrum with two Gaussians fitted. Middle panel shows the mean Stokes V spectrum for the four hyperfine components that have strong Zeeman splitting coefficients Z; the bottom panel shows the three components with weak Z. B_{los} was fitted independently for the two Gaussian lines.

3 An Observational Exemplar – DR21OH

Figure 1 shows results for the high-mass star formation region DR21OH; all three of the observational techniques discussed above have been employed. In millimeter-wave dust emission the main component of DR21OH consists of two compact cores with a total mass of ~ 100 $M_\odot$ (Woody et al. 1989). The two CN velocity components are each centered on a different one of the two compact cores. The region has signposts of high-mass star formation: masers of OH (Norris et al. 1982) and H_2O (Genzel & Downes 1977), and high-velocity outflows powered by the two compact cores (Lai et al. 2003), but as yet no well-developed H II regions. The results from the dust and CO 2-1 linear polarization maps suggest that the magnetic field direction in DR21OH is parallel to the CO polarization and therefore parallel to the major axis of DR21OH. This could be explained by a toroidal field produced by rotation of the double core. The CO and dust polarization maps suggest that magnetic fields are remarkably uniform throughout the region. Both the dust emission and the CN lines sample a density $n(H_2) \approx 1 \times 10^6$ cm^3. The Chandrasekhar-Fermi technique yields $B_{pos} \approx 1$ mG, compared with $B_{los} = -0.4 \pm 0.1$ mG and $B_{los} = -0.7 \pm 0.1$ mG inferred from the CN Zeeman detections shown in Fig. 1. Combining these results, $B_{total} \approx 1.1$ mG and $\mathbf{B}$ is at an angle $\theta \sim 60°$ to the line of sight. However, uncertainties in B_{pos} and B_{los} are sufficiently large that θ is quite uncertain. In general such complete information about $\mathbf{B}$ is not available and a statistical approach is necessary.

4 Observational Tests

4.1 Morphology

In the magnetic support model, the dominant **B** means field lines should be smooth, without irregular structure. Clouds will be thin disks or oblate spheroids, since thermal pressure provides the only support along field lines. The field lines should be parallel to the minor axes of clouds. Finally, an original morphology with parallel magnetic field lines will be transformed into an hourglass morphology since it is the tension of the bent field lines that provides support. In the turbulent model, **B** will be too weak to resist twisting by the dominant turbulence, and field lines will not be smooth but chaotic, with small-scale irregular structure. No correlation with cloud morphology is expected.

Maps of dust and spectral-line linear polarization and of the Zeeman effect generally show a regular field morphology (e.g., Fig. 1), and an hourglass morphology is sometimes seen (e.g., Schleuning 1998). A regular field dominating a random field and an hourglass morphology toward cores are predictions of the strong magnetic field model. However, **B** projected onto the sky is not observed to be parallel to the minor axes of starless cores as predicted by magnetic support (e.g., Ward-Thompson et al. 2000). Finally, even though fairly small, a significant small-scale dispersion in polarization position angles is often seen (e.g., Crutcher et al. 2004), implying that turbulence is producing an irregular component to **B**.

4.2 Scaling

The scaling of $|\mathbf{B}|$ with density ρ is usually parameterized as $|\mathbf{B}| \propto \rho^{\kappa}$, so our discussion will be in terms of κ. Since the ambipolar diffusion timescale is much shorter in a core than in an envelope, the core will become supercritical and collapse while the envelope remains subcritical and supported by the field. Hence, $|\mathbf{B}|$ in cloud envelopes remains virtually unchanged, so at lower densities no strong correlation between $|\mathbf{B}|$ and density ρ is predicted, and $\kappa \sim 0$. As ambipolar diffusion increases M/Φ in a core, ρ increases faster than $|\mathbf{B}|$; $\kappa \leq 0.5$ is predicted. In turbulent models, in the low-density case before gravity becomes important no relation is expected between the magnetic field strength and density; so again, on average, $\kappa \sim 0$. If a cloud becomes self-gravitating but the magnetic field is very weak, an approximately spherical collapse is expected, in which case $\kappa = 2/3$ is predicted (Mestel 1966).

At low densities $n \sim 0.1 - 100$ cm^{-3}, it has been clear for some time that there is no correlation of $|\mathbf{B}|$ with ρ (Troland and Heiles 1986), as both the turbulence and magnetic support models predict. At higher densities one finds $\kappa = 0.47 \pm 0.08$ (Crutcher 1999). This κ agrees with the ambipolar diffusion prediction and not with the very weak field, spherical collapse prediction.

4.3 Mass-to-flux ratio

The ratio of the mass in a magnetic flux tube to the magnitude of the magnetic flux is a crucial parameter for the magnetic support/ambipolar diffusion model. Since magnetically supported clouds will be thin disks, the relevant critical M/Φ where gravity is balanced by magnetic pressure is that for a uniform disk, which is $(M/\Phi)_{crit} = [2\pi\sqrt{G}]^{-1}$ (Nakano and Nakamura 1978). It is convenient to state M/Φ in units of the critical value, and to define $\lambda \equiv (M/\Phi)_{actual}/(M/\Phi)_{crit}$. Inferring λ from observations is possible if the column density

N and the magnetic field strength $|\mathbf{B}|$ are measured:

$$\lambda = \frac{(M/\Phi)_{observed}}{(M/\Phi)_{crit}} = \frac{mNA/|\mathbf{B}|A}{1/2\pi\sqrt{G}} = 7.6\times10^{-21}\frac{N(H_2)}{|\mathbf{B}|}, \tag{3}$$

where $m = 2.8m_H$ allowing for He, A is the cloud area of the observations, $N(H_2)$ is in cm^{-2}, and $|\mathbf{B}|$ is in μG.

If $\mathbf{B}$ is strong, clouds will have a disk morphology with $\mathbf{B}$ along the minor axis. To properly measure λ, one needs B and N along a flux tube, i.e., parallel to the minor axis. As noted by Crutcher (1999), the path length through a disk will be too long by $1/\cos\theta$ and N (and M) will be overestimated, while $|\mathbf{B}|$ (and Φ) will be underestimated by $\cos\theta$. Statistically, the mean over a large number of random θs is

$$\overline{M/\Phi} = \int_0^{\pi/2}\frac{M_{obs}\cos\theta}{\Phi_{obs}/\cos\theta}\sin\theta d\theta = \int_0^{\pi/2}(M/\Phi)_{obs}\cos^2\theta\sin\theta d\theta = \frac{1}{3}(M/\Phi)_{obs}. \tag{4}$$

It turns out that the same correction factor applies when the measurements are of B$_{pos}$. For any cloud geometry a correction of 1/2 must be applied (eq. 1). We will discuss λ_C obtained by applying the full correction factor of 1/3 to the directly observed λ, since a disk morphology is the prediction of the ambipolar diffusion model; the 1/3 correction must be applied to test this model.

In the ambipolar diffusion model clouds are initially subcritical, $\lambda < 1$. Ambipolar diffusion is fastest in shielded, high-density cores, so cores become supercritical, and rapid collapse ensues. The envelope continues to be supported by the magnetic field. Hence, the prediction is that λ must be < 1 in cloud envelopes, while in cores $\lambda \approx 1$. After a core becomes supercritical, $\lambda > 1$ would be observed; however, the collapse phase has a very short lifetime, so few cores with $\lambda > 1$ should be found. Hence, this model tightly constrains λ. On the other hand, the turbulent model imposes no direct constraints on λ, although strong magnetic fields would resist the formation of gravitationally bound clouds by compressible turbulence. Also, if magnetic support is to be insufficient to prevent collapse of self-gravitating clumps that are formed by compressible turbulence, the field must be supercritical, $\lambda > 1$. λ may take any value > 1, although of course for the turbulence model with very weak magnetic fields that we are considering, clouds will be highly supercritical, $\lambda >> 1$.

Figure 2 shows all of the λ_C available from Zeeman detections and sensitive limits for molecular clouds (Crutcher 1999; Bourke et al. 2001; Troland & Crutcher 2005), plus the Chandrasekhar-Fermi results for three prestellar cores (Crutcher et al. 2004). The observations are distributed roughly equally above and below the $\lambda_C = 1$ line that divides subcritical and supercritical M/Φ ratios for disk geometries. Therefore, the data suggest that $\overline{\lambda} \approx 1$; that is, the typical mass to magnetic flux ratio is approximately critical. There is a slight indication that for large column densities, $\overline{\lambda}$ may be supercritical, and for small column densities, subcritical. Since most of the observations that went into Fig. 2 are of cores, the data are consistent with the ambipolar diffusion model, which predicts $\lambda \approx 1$ for cores.

It is also relevant to consider mass-to-flux ratios in H I clouds, from which molecular clouds presumably form. Heiles and Troland (2004) have carried out an extensive study with the Arecibo telescope of Galactic H I clouds (for which $n(H\ I) \sim 50$ cm^{-3}) in absorption against background extragalactic continuum sources (see also Troland 2004). Their plot of B_{los} *vs.* $N(H\ I)$ showed that for all of the detections, the field was significantly subcritical. Moreover, almost all of the non-detections were also consistent with $\lambda < 1$. If these points

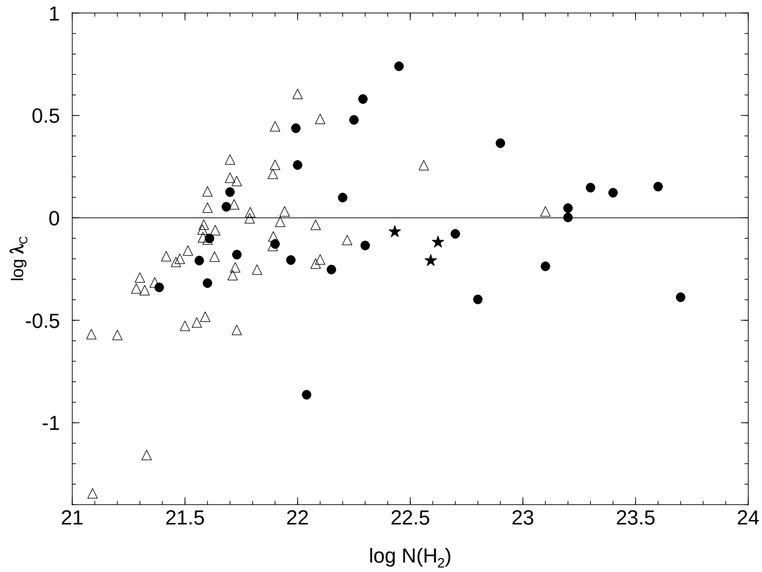

Figure 2: λ_C are the observed mass to magnetic flux ratios (eq. 3), divided by 3 to correct for projection bias (eq. 4), in units of the critical values. $\lambda_C > 1$ is supercritical, $\lambda_C < 1$ is subcritical. Dots are for Zeeman data with $B_{los} > 3\sigma(B_{los})$, stars are for Chandrasekhar-Fermi estimates of B_{pos}, and triangles are lower limits plotted at $B_{los} = 3\sigma(B_{los})$. Although the statistical correction of $1/3$ for geometrical bias has been applied to each point, so that statistically this plot should be valid, for any individual point the true λ could be higher or lower than the plotted λ_C. A large part of the scatter in this figure may therefore be due to geometrical projection effects.

were to be plotted on Fig. 2, they would lie to the left of and below the $\lambda_C = 1$ line (see Troland 2004). Hence, the H I data suggest that the precursors to molecular clouds are subcritical, as required by the magnetic support model.

The change in λ from subcritical values in diffuse clouds to critical ones in molecular cores probably takes place during the molecular cloud formation process. The observations toward dark cloud cores by Crutcher et al. (1993) sampled mainly the envelope regions of the dark clouds since the core diameters are typically $\sim 2'$ while the telescope beam diameter was $18'$; the typical density sampled was n(H_2) $\sim 10^3$ cm^{-3}, and λ was already approximately critical. The increase in λ between n(H I) ~ 50 cm^{-3} and n(H_2) $\sim 10^3$ cm^{-3} may have been produced by material accumulating along flux tubes to form dense clouds (e.g., Hartmann et al. 2001); although this would not actually increase the mass to flux ratio in a flux tube, observers of individual H I clouds in the flux tube would infer a lower λ than would be found after H I clouds aggregate to form a single dense molecular cloud.

5 Conclusions

The generally regular morphology of polarization maps supports a strong magnetic field model. Yet the small-scale scatter in polarization position angles predicted by turbulence is seen, although this scatter is generally relatively small. As projected onto the sky, **B** is not parallel to the minor axes of cores, as predicted by the magnetic support model. A triaxial cloud morphology, due perhaps to formation by compressible turbulence, can account for this (Basu 2000). In molecular clouds the observed scaling of $|\mathbf{B}|$ versus ρ with a power-law index of $\kappa = 0.47 \pm 0.08$ agrees with the ambipolar diffusion prediction and not with the weak $|\mathbf{B}|$ prediction of $\kappa = 2/3$. The observations of molecular cloud cores are consistent with $\lambda \approx 1$. This is certainly inconsistent with the extreme turbulent model with negligible **B**, for which $\lambda >> 1$. Although $\lambda \approx 1$ is predicted to occur in cores as a result of ambipolar diffusion when the original mass-to-flux ratio was subcritical, the observational evidence for subcritical molecular clouds and envelopes is weak. Whether λ is slightly greater than or slightly less than 1 is crucial for whether magnetic fields provide support that is removed by the action of ambipolar diffusion. The present data are not sufficiently accurate to discriminate between these cases.

It seems that the data remain inconclusive in deciding between the two models for what drives star formation. However, the fact that the regular component of **B** seems to dominate the irregular component, that $\kappa \neq 2/3$, and that mass-to-flux ratios are approximately critical ($\lambda \approx 1$) rather than the highly supercritical ($\lambda >> 1$) values predicted by weak field models supports for the strong magnetic field model. A hybrid paradigm may be closest to the truth. In such a paradigm, compressible turbulence dominates in the diffuse ISM over both gravity and magnetic fields, sometimes forming self-gravitating clouds. Since magnetic fields are observed to be strong, the turbulent flow would be primarily along flux tubes. Aggregation of individually subcritical H I clouds into a single molecular cloud would lead to the observed apparent increase in the mass to flux ratio. The residual effects of this turbulence are seen in self-gravitating molecular clouds, but such clouds appear to be approximately magnetically supported. In any case, it seems clear that *both* turbulence and strong magnetic fields are important in the physics of molecular clouds.

As is often the case in astronomy, further observations are needed. Tests of the role of magnetic fields are of necessity statistical in nature and must involve data covering a wide range of physical parameters. Required are additional high sensitivity surveys of magnetic field strengths and other cloud properties in order to assess the relative importance of magnetic fields in molecular cores and envelopes. These surveys should include extended polarization maps that allow a determination of how the field in the cores connects with that in its surroundings. But the single most crucial observation that is needed is the measurement of magnetic field strengths in a statistically significant sample of molecular cloud envelopes. If envelopes are subcritical, for a large sample at least some of the fields must be nearly along the line of sight, and Zeeman observations will detect unambiguous subcritical mass-to-flux ratios. Clear evidence for an increase in the mass-to-flux ratio from envelope to core would then verify the ambipolar diffusion model. Alternatively, if future observations show that this is not the case, turbulence driven star formation (although with dynamically important magnetic fields) would be favored. Future telescopes and instruments will enable ever more sensitive and extensive observations that hopefully will define more precisely the role of magnetic fields in the star formation process.

Acknowledgments

This work was partially supported by NSF grant AST 02-05810. I thank Tom Troland for an enjoyable and productive collaboration on the study of interstellar magnetic fields.

References

Basu, S., 2000, ApJ, 540, L103

Bourke, T. L., Myers, P. C., Robinson, G., Hyland, A. R., 2001, ApJ, 554, 916

Chandrasekhar, S., Fermi, E., 1953, ApJ, 118, 113

Crutcher, R. M., Troland, T. H., Goodman, A. A., Heiles, C., Kazès, I., Myers, P. C., 1993, ApJ, 407, 175

Crutcher, R.M., Troland, T.H., Lazareff, B., Paubert, G., Kazès, I., 1999, ApJ, 514, L121

Crutcher, R. M., 1999, ApJ, 520, 706

Crutcher, R. M., Nutter, D., Ward-Thompson, D., Kirk, J. M., 2004, ApJ, 600, 279

Elmegreen, B.G., 2000, ApJ, 530, 277

Genzel, R., Downes, D., 1977, AApS, 30, 145

Goldreich, P., Kylafis, N.D., 1981, ApJ, 243, L75

Hartmann, L., Ballesteros-Paredes, J., Bergin, E. A., 2001, ApJ, 562, 852

Heiles, C., Troland, T.H., 2004, ApJS, 151, 271

Kylafis, N. D., 1983, ApJ, 275, 135

Lai, S.-P., Girart, J.M., Crutcher, R.M., 2003, ApJ, 598, 392

Lazarian, A., 2003, JQSRT, 79, 881

MacLow, M.-M., Klessen, R.S., 2004, Rev. Mod. Phys., 76, 125

Mestel, L., 1966, MNRAS, 133, 265

Mouschovias, T. Ch., Ciolek, G. E., 1999, in *The Origin of Stars and Planetary Systems*, ed. C. J. Lada & N. D. Kylafis (Kluwer), p. 305

Nakano, T., Nakamura, T., 1978, PASJ, 30, 681

Norris, R.P., Booth, R.S., Diamond, P.J., Porter, N.D., 1982, MNRAS, 201, 191

Ostriker, E. C., Stone, J. M., Gammie, C. F., 2001, ApJ, 546, 980

Schleuning, D. A., 1998, ApJ, 493, 811

Troland, T.H., Crutcher, R.M., 2005, to be submitted to ApJ

Troland, T. H., Heiles, C., 1986, ApJ, 301, 339

Troland, T.H., 2004, in *The Magnetized Interstellar Medium*, eds. B. Uyaniker, W. Reich, R. Wielebinski (Copernicus GmbH), p. 105

Ward-Thompson, D., Kirk, J.M., Crutcher, R.M., Greaves, J.S., Holland, W.S., & André, P., 2000, ApJ, 537, L135

Woody, D.P., Scott, S.L., Scoville, N.Z., Mundy, L.G., Sargent, A.I., Padin, S., Tinney, C.G., Wilson, C.D., 1989, ApJ, 337, L41